Available online at www.sciencedirect.com
SCIENCE DIRECT®
ELSEVIER
International Journal of Multiphase Flow 30 (2004) 327–345
International Journal of Multiphase Flow
www.elsevier.com/locate/ijmulflow

Focus on the dispersed phase boundary conditions at the wall for irregular particle bouncing

A. Tanière, M. Khalij, B. Oesterlé *

LEMTA—UMR 7563 CNRS, ESSTIN, Université Henri Poincaré, 2 rue Jean Lamour, 54519 Vandoeuvre-lès-Nancy, France

Received 31 July 2003; received in revised form 28 October 2003

Abstract

The dispersed phase wall boundary conditions for gas–particle flows are investigated here accounting for the effects of wall roughness on frictional inelastic particle–wall collisions. Particle statistics at the wall are computed by simulating a large number of particle–wall impacts for a given distribution of the incident wall normal velocity. The collisions are treated by using an irregular bouncing model and avoiding unphysical impact or reflected angles, the so-called shadow effect. In this sense, the present study is a preliminary step towards improvement of the formulation of wall boundary conditions for the dispersed phase needed in two-fluid models. The current approaches which allow deriving the dispersed phase boundary conditions in the cases of smooth and rough wall are described and analyzed. By taking the zero mass flux condition and the shadow effect into account, the second- and third-order particle velocity correlations at the wall can be compared to the theoretical relations obtained in the smooth case. Equivalent friction and restitution coefficients are defined, making it possible to use the same formulation of the dispersed phase boundary conditions as established in the smooth wall case. The dependence of these equivalent coefficients upon the actual collision parameters and the wall roughness is illustrated by the results of the numerical simulation.

Keywords: Gas–solid flow; Particle–wall collisions; Wall roughness; Boundary conditions

1. Introduction

Generation and transport of powders in the chemical and pharmaceutical industries, in turbulent combustion sprays, sedimentation of dilute suspensions are all examples of particle–laden

* Corresponding author. Tel.: +33-383-685-080; fax: +33-383-685-085.
E-mail addresses: taniere@esstin.uhp-nancy.fr (A. Tanière), benoit.oesterle@esstin.uhp-nancy.fr (B. Oesterlé).

0301-9322/$ - see front matter
doi:10.1016/j.ijmultiphaseflow.2003.11.013

flows. Confined gas–solid flows are frequently found in industrial process technology. Nowadays, two approaches are mainly used for the numerical prediction of dispersed two-phase flows. In the so-called Lagrangian method the discrete elements are tracked through a turbulent fluid field by solving their equations of motion. In the second methodology, both phases are handled as two interpenetrating continuums and are governed by a set of differential equations representing conservation laws; this approach is known as Eulerian–Eulerian or two-fluid model. Although such models are more effective and less time consuming than Lagrangian simulations, traditional closures may fail in accurate predictions of the dispersed phase turbulent quantities. To overcome this, considerable efforts have been dedicated during the past years to the development of second-order turbulence closures for the particulate phase (Reeks, 1993; Simonin et al., 1993; Hyland et al., 1998; Zhou et al., 2001). Those topics are still in the research stage specially as concerns the particulate phase wall conditions. It is easier to take the presence of the wall into account by Lagrangian simulation just by the use of rebound laws and introducing the effect of particle shape or wall roughness by means of a virtual wall model (Tsuji et al., 1987; Sommerfeld, 1992; Sommerfeld and Huber, 1999). In two-fluid models, the wall exists only through the boundary conditions needed for the solution of the differential system. In order to obtain accurate information about the influence of the wall on the behaviour of solid particles, it is important to develop a set of boundary conditions for the dispersed phase. The establishment of boundary conditions incorporating the effect of wall roughness is identified as one of the objectives pursued in this paper.

The usual approach to establish boundary conditions for the dispersed phase in two-fluid models is based on the determination of the probability density function (PDF) of the particle velocities close to the wall. Using this PDF-two-fluid method, the mean value of any variable at the wall can be expressed as a function of the mean value before collision, and relationships between the various statistical moments of the particle velocity components can be derived, provided that a deterministic rebound law is prescribed. This method was applied by He and Simonin (1993) and Sakiz and Simonin (1999) in order to obtain the dispersed phase boundary conditions at a smooth wall in terms of the Coulomb parameters (coefficients of friction and restitution), using a pre-assigned binormal PDF for the wall normal particle velocity. Another approach, based on solving the kinetic equation for the particle velocity PDF, was described and discussed by Alipchenkov et al. (2001), however in this method the velocity distribution is assumed to be Gaussian, and the range of variation of the collision parameters is restricted.

The above cited methods are dedicated to the case of a smooth wall. The roughness of the wall is known to be essential for simulations of gas–particle confined flows (like channel or pipe flows) in order to obtain realistic spatial distributions of the particles (Tsuji et al., 1985). The roughness of the wall is responsible for the redistribution of momentum components of particles without excessive accumulation in the vicinity of the wall due to collisions. However, few works exist taking the effect of wall roughness into account in order to derive the dispersed phase boundary conditions at the wall, except the recent work of Zhang and Zhou (2002) based on the PDF-two-fluid method. With the help of a virtual wall model (Sommerfeld, 1992), they constructed a particle–wall interaction model for second-order two-phase turbulence methods, depending on the friction and restitution coefficients, and gave analytical relations describing the influence of the wall roughness on the particle boundary conditions. However, the use of the virtual wall model without performing some tests based on the generated values of the virtual wall inclination is not

recommended (Sommerfeld and Huber, 1999). Some generated angles can be unphysical and must be eliminated in order to obtain a realistic simulation of the particle–wall interaction. This effect, called the shadow effect, is not taken into account in the work of Zhang and Zhou (2002). Moreover, they indicate that the introduction of roughness in their study can result in nonzero normal mean velocity, i.e. the particle mass flux at the wall is not equal to zero. The main objective of the present investigation is to correct such a drawback and thus complement their work. For this purpose, we use the approach proposed by He and Simonin (1993) and Sakiz and Simonin (1999), who obtained the dispersed phase boundary conditions at a smooth wall under the form of theoretical relationships involving the second- and third-order particle velocity correlations and depending on the wall normal velocity distribution. The velocity moments at the wall are estimated by means of Dirichlet and flux conditions. The latter uses a diffusion model expressing the third-order correlations as a function of the second-order correlations, for which Dirichlet conditions are given. Thus, the third-order wall normal particle velocity correlations have to be evaluated by another means. Some assumption on the PDF of the incident normal velocity of the particles has to be made. A priori, such incident particle velocities are unknown in a channel or pipe flows for example, where the particle motion is governed by a number of other physical effects, such as turbulence which can modify the incident velocity distribution if the particles are subject to such influences.

In order to dissociate these two contributions, a statistical study on a large number of particle rebounds at the wall is carried out with prescribed forms of the incident particle velocity PDF. Roughness is introduced in the numerical simulations by means of the virtual wall model of Sommerfeld (1992), taking the shadow effect into account by eliminating unphysical inclination angles of the wall. Before presenting and discussing the numerical simulations, the formalisms used in the cases of smooth wall and rough wall are described and compared, with the objective to investigate whether corrections of the relations obtained in the smooth wall case are possible. Equivalent restitution and friction coefficients are introduced and their dependence on the roughness parameter is studied.

2. Theoretical considerations for a smooth wall

2.1. The formalism used by Sakiz and Simonin (1999) for the derivation of smooth wall boundary conditions

The reader is referred to Sakiz and Simonin (1999) for the details of their analysis based on the kinetic theory formalism. The smooth and plane wall is supposed to be normal to the y-direction as shown in Fig. 1. The instantaneous velocity vector of a spherical solid particle before and after impact are denoted by $\mathbf{u}$ and $\tilde{\mathbf{u}}$, respectively. The incident particles have a negative wall normal velocity component, $\mathbf{u}\cdot\mathbf{n} = u_Y$, where $\mathbf{n}$ is the unit vector normal to the wall (parallel to the y-axis), and the reflected particles have a positive velocity component as shown in Fig. 1. The main assumptions are as follows:

- The particle statistics are stationary and homogeneous in the x-direction.
- The rebounds are deterministic and instantaneous, therefore the reflected velocity does not

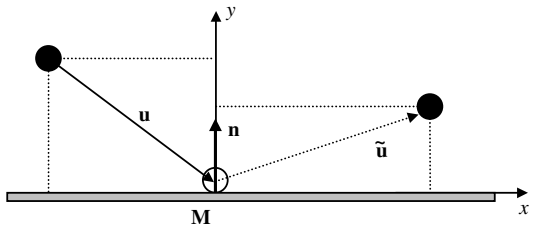

Fig. 1. Sketch of the rebound of a particle on a plane wall.

depend on any aerodynamic force (like the Magnus effect) which may affect the particle motion after a collision, but which cannot influence the boundary conditions under investigation.

- Sliding is assumed to occur during every collision.
- The particle velocity component in the spanwise direction is negligible compared to the x-component, so that the problem can be handled in a two-dimensional way. It must be pointed out that this hypothesis does not mean that the particle rotational motion is neglected, because only the x-component of the angular velocity has to be neglected to obtain such collisions where the reflected velocity lies in the plane formed by the incident velocity vector and the y-axis.

Under these assumptions, the equations governing the translational and rotational velocity components are fully disconnected (see Sakiz and Simonin, 1999).

Using a distribution function f for the velocity of the particles, the mean value of any function ψ of the velocity is given by

$$\langle \psi(\mathbf{u}) \rangle = \frac{1}{N} \int \psi(\mathbf{u}) f(\mathbf{u}) \, \mathrm{d}\mathbf{u}, \tag{1}$$

where $N = \int f(\mathbf{u}) \, \mathrm{d}\mathbf{u}$ is the particle number density at the wall. The fluctuation of ψ is defined by $\psi' = \psi - \langle \psi \rangle$. In order to focus on the effect of the rebounds on the wall, Sakiz and Simonin (1999) distinguish the mean values of ψ for incident $\langle \, \rangle^-$ and reflected particles $\langle \, \rangle^+$, linked by the following relation:

$$N \langle \psi \rangle = N^- \langle \psi \rangle^- + N^+ \langle \psi \rangle^+, \tag{2}$$

where N^- and N^+ are the number densities of incident and reflected particles at the wall, respectively, so that $N = N^- + N^+$. Eq. (2) can be written using the parameter ξ defined by $\xi = N^-/N$:

$$\langle \psi \rangle = \xi \langle \psi \rangle^- + (1 - \xi) \langle \psi \rangle^+. \tag{3}$$

As the rebounds are assumed to be purely deterministic, a rebound law function ϕ which links the incident and reflected velocities of the particle at the wall can be introduced: $\tilde{\mathbf{u}} = \phi(\mathbf{u})$.

In the wall normal direction, the bouncing is supposed to obey $\tilde{\mathbf{u}} \cdot \mathbf{n} = -e\mathbf{u} \cdot \mathbf{n}$, where e is the coefficient of restitution in the wall normal direction. Therefore, the condition of zero mass flux at the wall, obtained by applying Eq. (3) to the wall normal velocity component, is

$$\xi_0 = \frac{e}{1+e}, \tag{4}$$

where ξ_0 is the value of the parameter ξ for a smooth wall.

By introducing the probability density function for a particle hitting the wall with velocity $\mathbf{u}$ to leave it with a new velocity in the range $[\tilde{\mathbf{u}}, \tilde{\mathbf{u}} + \mathrm{d}\tilde{\mathbf{u}}]$, Sakiz and Simonin (1999) derived the following expression of the velocity distribution function of the reflected particles, f^+, as a function of the distribution function of the incident particles, f^-:

$$f^+(\tilde{\mathbf{u}}) = \frac{1}{eJ_\phi} f^-(\phi^{-1}(\tilde{\mathbf{u}})), \tag{5}$$

where J_ϕ is the Jacobian of ϕ. The main advantage of this formula is that the function f^+ is calculated making assumptions only on f^-. From Eqs. (3)–(5), the main relationship used to obtain the wall boundary conditions can be shown to be

$$\langle \psi(\mathbf{u}) \rangle = \frac{e}{1+e} \langle \psi(\mathbf{u}) \rangle^- + \frac{1}{1+e} \langle \psi(\tilde{\mathbf{u}}) \rangle^-, \tag{6}$$

where $\mathbf{u} = \phi^{-1}(\tilde{\mathbf{u}})$. The rebound law ϕ has to be given in order to complement the model.

In order to express the particle translational velocity after the collision, the impulsive equations and Coulomb's law are used. Besides the coefficient of restitution e, the rebound law is therefore expressed by means of the friction factor μ. In the case where sliding occurs in the longitudinal direction, and under the above-mentioned condition of negligible spanwise component of the impact velocity for all particles, the mechanical rebound laws for the translational velocity components are

$$\begin{cases} \tilde{u}_X = u_X + \mu(1+e)u_Y, \\ \tilde{u}_Y = -eu_Y, \\ \tilde{u}_Z = u_Z (= 0), \end{cases} \tag{7}$$

or, in matrix form

$$\tilde{\mathbf{u}} = \mathbf{Q}\mathbf{u} \quad \text{with} \quad \mathbf{Q} = \begin{bmatrix} 1 & \mu(1+e) & 0 \\ 0 & -e & 0 \\ 0 & 0 & 1 \end{bmatrix}. \tag{8}$$

As mentioned above, the relationships involving the angular velocities of the particles are disconnected from the equations giving the translational velocity components, thus making it possible to focus on the statistical moments of the translational velocity components which are needed to express the boundary conditions for Eulerian models, keeping in mind that such models are still unable to deal with the rotational motion of particles.

2.2. Dispersed phase boundary conditions at a smooth wall

By means of Eqs. (6) and (7), Sakiz and Simonin (1999) derived the following relationships expressing the various moments of the particle velocity components at the wall in terms of the only unknown $\langle u_Y'^3 \rangle^-$:

$$\left.\begin{array}{l} \langle u_Y \rangle = 0 \\ \langle u'_X u'_Y \rangle = -\mu \langle u'^2_Y \rangle \\ \langle u'^2_X u'_Y \rangle = -2\mu \langle u'_X u'^2_Y \rangle - \mu^2 e(1-e) \langle u'^3_Y \rangle^- \\ \langle u'^3_Y \rangle = e(1-e) \langle u'^3_Y \rangle^- \end{array}\right\}. \tag{9}$$

In order to obtain an estimation of $\langle u'^3_Y \rangle^-$, which is required to close this set of equations, it is necessary to make an assumption about the distribution of the wall normal incident particle velocity, defined by

$$f^-_Y(u_Y) = \int f^-(\mathbf{u})\, \mathrm{d}u_X\, \mathrm{d}u_Z, \tag{10}$$

which has the following properties:

$$\int_{-\infty}^{0} f^-_Y(u_Y)\, \mathrm{d}u_Y = N^-, \quad \int_{-\infty}^{0} u^2_Y f^-_Y(u_Y)\, \mathrm{d}u_Y = N^- \langle u'^2_Y \rangle^-. \tag{11}$$

Several distributions of the wall normal incident particle velocity can be tested. For a Gaussian distribution of f^-_Y (as used by Sakiz and Simonin, 1999),

$$f^-_Y(u_Y) = \frac{2N^-}{\sqrt{2\pi \langle u'^2_Y \rangle^-}} \exp\left(-\frac{u^2_Y}{2\langle u'^2_Y \rangle^-} \right), \tag{12}$$

the following expression is obtained for $\psi = u'^3_Y$ by means of relations (1) and (12):

$$\langle u'^3_Y \rangle^- = -\frac{4}{\sqrt{2\pi}} [\langle u'^2_Y \rangle^-]^{3/2}. \tag{13}$$

In the case where the distribution of the wall normal incident particle velocity is assumed to be uniform (in the range $[-\sqrt{3\langle u'^2_Y \rangle^-}, +\sqrt{3\langle u'^2_Y \rangle^-}]$ in order that the variance remains equal to $\langle u'^2_Y \rangle^-$), f^-_Y is expressed by

$$f^-_Y(u_Y) = \frac{1}{2\sqrt{3\langle u'^2_Y \rangle^-}}, \tag{14}$$

which yields

$$\langle u'^3_Y \rangle^- = -\frac{3\sqrt{3}}{4} [\langle u'^2_Y \rangle^-]^{3/2}. \tag{15}$$

More generally, for any distribution of the wall normal incident velocity, we can introduce the constant C defined by

$$\langle u'^3_Y \rangle^- = C[\langle u'^2_Y \rangle^-]^{3/2}. \tag{16}$$

Using the relation $\langle u'^2_Y \rangle^- = \frac{1}{e} \langle u'^2_Y \rangle$, obtained by means of Eqs. (6) and (8) for $\psi = u'^2_Y$, the dispersed phase boundary conditions can finally be obtained as

$$\left.\begin{aligned}
&\langle u_Y\rangle = 0\\
&\langle u'_X u'_Y\rangle = -\mu\langle u'^2_Y\rangle\\
&\langle u'^2_X u'_Y\rangle = -2\mu\langle u'_X u'^2_Y\rangle - \mu^2\langle u'^3_Y\rangle\\
&\langle u'^3_Y\rangle = C\tfrac{1-e}{\sqrt{e}}\langle u'^2_Y\rangle^{3/2}
\end{aligned}\right\}, \tag{17}$$

where C depends on the distribution of u_Y.

The presented formalism is based on purely deterministic rebounds, which means that it cannot be applied for stochastic rebounds which may occur as a consequence of the roughness of the wall. As mentioned in the introductory section, the only available work on this subject is due to Zhang and Zhou (2002), who proposed wall boundary conditions for the dispersed phase to be used in a second-order two-phase turbulence model for two-dimensional flows, accounting for the roughness of the wall. In the next section, the rebound laws taking into account the roughness of the wall are first presented. The formalism used by Zhang and Zhou (2002) is then discussed and analyzed.

3. Formalism for the rough wall case

3.1. Rebound law accounting for wall roughness

The effect of wall roughness can be introduced into the previous relations (8) by means of the so-called "virtual wall" model of Sommerfeld (1992). In this model, the actual wall is replaced by a virtual wall, whose inclination angle γ obeys a Gaussian distribution function with a given standard deviation σ_γ and a zero mean value as shown in Fig. 2. The velocity components in the virtual wall co-ordinate system are

$$\begin{cases} \tilde{\mathbf{u}}_{|x,y} = \mathbf{P}\,\tilde{\mathbf{u}}_{|X,Y} \\ \mathbf{u}_{|x,y} = \mathbf{P}\,\mathbf{u}_{|X,Y} \end{cases} \quad \text{with} \quad \mathbf{P} = \begin{bmatrix} \cos\gamma & \sin\gamma & 0 \\ -\sin\gamma & \cos\gamma & 0 \\ 0 & 0 & 1 \end{bmatrix}. \tag{18}$$

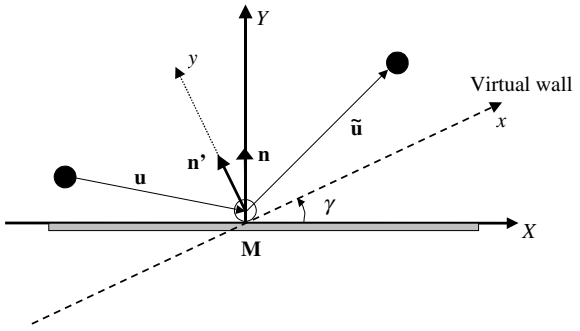

Fig. 2. The virtual wall model.

According to (8) and (18), the post-collisional components with respect to the fixed co-ordinates X and Y become

$$\tilde{\mathbf{u}}_{|X,Y} = \mathbf{P}^{-1}\mathbf{Q}\mathbf{P}\,\mathbf{u}_{|X,Y}. \tag{19}$$

Attention must be paid to the validity of such rebound laws. Sommerfeld and Zivkovic (1992), Schade and Hadrich (1998) and Sommerfeld and Huber (1999) have shown that the distribution of the inclination angle depends on the impact angle of the particle with respect to the wall (the so-called shadow effect). In order to simulate a physical rebound, some values of the virtual wall inclination angle γ must be avoided, because the incident and the reflected velocities must satisfy $u_y < 0$ and $\tilde{u}_Y > 0$, respectively. Fig. 3(a) illustrates the shadow effect in the case of an incident particle with impact angle α_i, for a random generated value of the wall inclination γ^*. As is obvious from this sketch, the collision with the virtual wall is impossible if $\alpha_I < -\gamma$ since in this case we would have $u_y > 0$. Similarly, another unphysical situation can appear considering the rebound after the impact as shown in Fig. 3(b) since we have $\tilde{u}_Y < 0$. (However, the latter situation could be treated as physically valid in a Lagrangian simulation if a second wall–particle collision is imposed just after the first impact.) Thus, testing the signs of $\mathbf{u} \cdot \mathbf{n}'$ and $\tilde{\mathbf{u}} \cdot \mathbf{n}$ (where $\mathbf{n}'$ is the unit vector normal to the virtual wall) allows accounting for the shadow effect by disregarding the unphysical cases in the numerical simulation.

As shown by Sommerfeld and Huber (1999), a consequence of the shadow effect is that the distribution function of γ is shifted towards the positive values. An example of such a distribution function obtained by numerical simulation, as explained further, is given in Fig. 4. As expected, a positive mean value of the wall inclination angle is clearly observed. Therefore, taking the shadow effect into account seems of importance in order to simulate realistic rebounds. However, up to now, the only work about Eulerian modelling of dispersed phase boundary conditions with wall roughness does not account for this effect. This work is by Zhang and Zhou (2002), who focused on the dispersed phase boundary conditions, but did not mention any test on unphysical impact and reflected angle values, assuming that the inclination of the wall is so small that they can neglect the shadow effect. Moreover, the distribution function f_γ of the virtual wall inclination angle was uniform, whereas the experimental measurements of wall roughness by Sommerfeld and Huber (1999) showed that a Gaussian distribution is more appropriate.

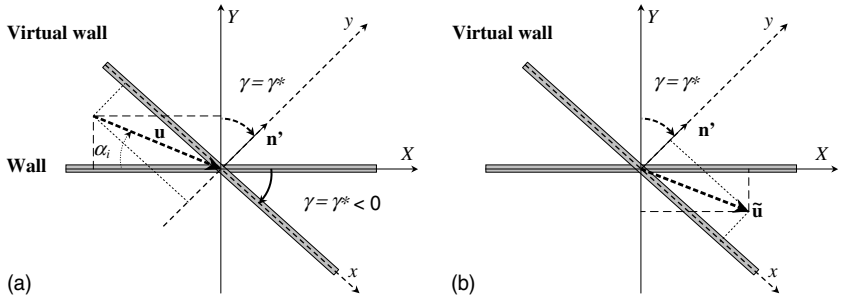

Fig. 3. Illustrations of unphysical inclination angles of the wall: (a) the incident shadow effect and (b) the reflected shadow effect.

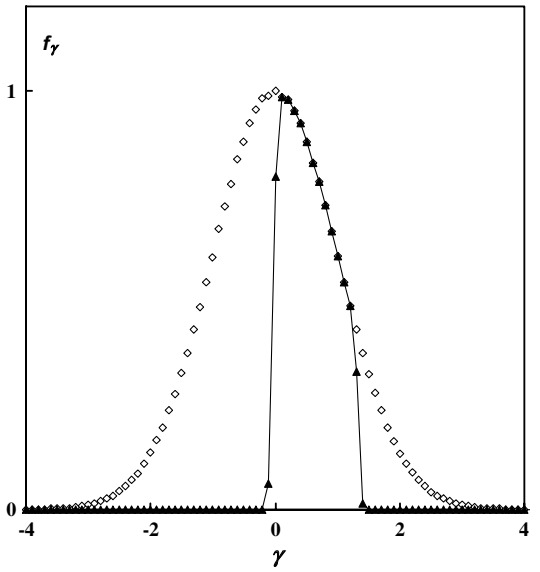

Fig. 4. Influence of the shadow effect on the distribution of the inclination angle of the wall for a Gaussian distribution of u_Y. $e = 0.8$, $\mu = 0.2$, $\langle u_X\rangle^- / \sqrt{\langle u_Y'^2\rangle^-} = 10$, $\sigma_\gamma = 0.2$. (◇) Original PDF of γ; (▲) PDF of γ after eliminating unphysical impact and reflected angles.

3.2. Comparison of the formalisms used for smooth and rough wall

The formalisms used in previous works are summarized in Table 1, which shows how Zhang and Zhou (2002) modified the initial formula (6) obtained by Sakiz and Simonin (1999) in order to apply it for a rough wall. Below, we discuss the formalism used by Zhang and Zhou (2002). As can be observed in Table 1, the starting relation (3) is the same. Such a relationship is true in any case (smooth and rough wall). It can be observed, however, that Zhang and Zhou (2002) used Eq. (6), which comes from Eq. (3) based on the assumption that the rebounds are deterministic, i.e. that any value of a reflected variable corresponds to one well defined value of the corresponding incident variable. In this sense, it is clear that Eq. (6) cannot be used in the case of a rough wall. Moreover, Zhang and Zhou (2002) used the value of ξ_0 obtained for a smooth wall where the ratio between N^+ and N^- is equal to $1/e$ an assumption which does not account for the effect of roughness on the ratio of particle number densities N^+/N^-. The particle mass flux at the wall has to be equal to zero, i.e. $\langle u_Y\rangle = 0$. The relation (3), written for $\psi = u_Y$, shows that the parameter ξ must therefore satisfy the following condition:

$$\xi = \frac{N^-}{N} = \frac{\langle \tilde{u}_Y\rangle^+}{\langle \tilde{u}_Y\rangle^+ - \langle u_Y\rangle^-}, \tag{20}$$

where $\langle \tilde{u}_Y\rangle^+$ is related to $\langle u_Y\rangle^-$ by the rebound law (keeping in mind that $\langle u_Y\rangle^- < 0$). According to Eq. (19), $\langle \tilde{u}_Y\rangle^+$ is related to $\langle u_Y\rangle^-$ by a function which depends on the Coulomb parameters and on the inclination angle of the virtual wall γ. Therefore, it is not surprising that ξ depends on these parameters. Eq. (20) ensures zero particle mass flux at the real wall, a physical boundary condition which is not satisfied in the derivation of Zhang and Zhou (2002).

Table 1
Comparison of the formalisms used for smooth and rough wall

Smooth wall: $\sigma_\gamma = 0$, Sakiz and Simonin (1999)	Rough wall: $\sigma_\gamma \neq 0$, Zhang and Zhou (2002)
Starting point: Eq. (3) $\langle\psi(\mathbf{u})\rangle = \xi\langle\psi(\mathbf{u})\rangle^- + (1-\xi)\langle\psi(\mathbf{u})\rangle^+$, where $\xi = \frac{N^-}{N}$, $N = N^- + N^+$ For $\psi = 1$, $N^+ = \frac{1}{e}N^-$ and $\xi_0 = \frac{e}{1+e}$	
Gaussian distribution for u_Y: $f_Y^-(u_Y) = \frac{2N^-}{\sqrt{2\pi\langle u_Y'^2\rangle^-}} \exp\left(-\frac{u_Y^2}{2\langle u_Y'^2\rangle^-}\right)$	Uniform distribution for u_Y: $f_Y^-(u_Y) = \frac{1}{2\sqrt{3\langle u_Y'^2\rangle^-}}$ for $-\sqrt{3\langle u_Y'^2\rangle^-} < u_Y < \sqrt{3\langle u_Y'^2\rangle^-}$
Resulting relation $\langle\psi(\mathbf{u})\rangle = \xi_0\langle\psi(\mathbf{u})\rangle^- + (1-\xi_0)\langle\psi(\tilde{\mathbf{u}})\rangle^-$	$\langle\psi(\mathbf{u})\rangle = \xi_0\langle\psi(\mathbf{u})\rangle^- + (1-\xi_0)\langle(\psi(\tilde{\mathbf{u}}))_\gamma\rangle^-$ with $(\psi)_\gamma = \int_{-\infty}^{+\infty}\psi f_\gamma(\gamma)\,\mathrm{d}\gamma$

3.3. Towards a more appropriate proposal

From the general expression of ξ given by Eq. (20), the correct asymptotic limit for the smooth wall case, where $\langle\tilde{u}_Y\rangle^+ = -e\langle u_Y\rangle^-$, is obviously obtained, namely,

$$\xi \to \xi_0 = \frac{e}{1+e} \quad \text{as } \sigma_\gamma \to 0. \tag{21}$$

In the rough wall case, we define an equivalent restitution coefficient e^* by

$$\langle\tilde{u}_Y\rangle^+ = -e^*\langle u_Y\rangle^- \tag{22}$$

in such a way that we obtain an expression of ξ similar to (4):

$$\xi = \frac{e^*}{1+e^*}, \tag{23}$$

where e^* is expected to depend not only on e, μ, σ_γ, but also on the statistical distribution of u_Y and on the ratio $\langle u_X\rangle/\sqrt{\langle u_Y'^2\rangle^-}$, which determines the distribution of the angle of incidence. Similarly, we propose an equivalent friction factor μ^*, using directly the formulation of the boundary condition obtained for the smooth wall case:

$$\mu^* = -\frac{\langle u_X' u_Y'\rangle}{\langle u_Y'^2\rangle}. \tag{24}$$

We then rewrite Eq. (3) in the following form, where the effects of the restitution coefficient, friction factor and roughness upon the particle phase boundary conditions at the wall are introduced via e^*:

$$\langle\psi\rangle = \frac{e^*}{1+e^*}\langle\psi\rangle^- + \frac{1}{1+e^*}\langle\psi\rangle^+. \tag{25}$$

Taking into account such equivalent Coulomb coefficients, a model is proposed for the particulate phase boundary conditions by analogy with (17), ensuring $\langle u_Y \rangle = 0$ at the wall:

$$\left.\begin{array}{l} \langle u_X'^2 u_Y' \rangle = -2\mu^* \langle u_X' u_Y'^2 \rangle - \mu^{*2} \langle u_Y'^3 \rangle \\ \langle u_Y'^3 \rangle = C \frac{1-e^*}{\sqrt{e^*}} \langle u_Y'^2 \rangle^{3/2} \end{array}\right\}, \tag{26}$$

where e^*, μ^* and C are defined by Eqs. (22), (24) and (16), respectively.

4. Numerical simulation, results and discussion

The main objective here is to numerically investigate the dependence of the equivalent coefficients e^* and μ^* upon the primary collision parameters, mainly the roughness parameter, for given distributions of the incident velocity, and to examine the suitability of the proposed model. For this reason, the numerical results about the dispersed phase boundary conditions at the wall are presented with comparison to the results issuing from the model (26). The collisions were assumed to be two-dimensional, i.e. the spanwise velocity of the particle was not taken into account ($u_Z = 0$). For each specification of the collision parameters, we simulated a large number of particle rebounds (10^6) by means of the rebound law (19). The distribution of the virtual wall inclination angle was Gaussian with given standard deviation σ_γ and zero mean value. The values of σ_γ tested here were varied from 0 to 0.2 according to the results of Sommerfeld and Huber (1999), who showed that the optimum value of σ_γ decreases with increasing particle diameter for a given physical roughness. The choice of the value of σ_γ in practical problems can be made according to the recent work by Sommerfeld (2003), who provided correlations of σ_γ as a function of the particle diameter ($0 < d_p < 500$ μm) for spherical particles. At the present time however, it is not clear how to decide the value of σ_γ in order to apply such an irregular bouncing model for nonspherical particles, although the results obtained by Sommerfeld (2002) by means of the exact impulse equations for various particle shapes are very promising in order to develop such a model.

The distributions of the incident velocity components were prescribed as follows:

- The calculations were performed for two distinct statistical distributions of the wall normal incident velocity of the particles, namely the Gaussian distribution used by Sakiz and Simonin (1999) and the uniform distribution used by Zhang and Zhou (2002).
- The tangential incident particle velocity was assumed to obey a Gaussian distribution with standard deviation equal to the wall normal one, i.e. $\langle u_X'^2 \rangle^- = \langle u_Y'^2 \rangle^-$. This is a strong assumption since in practical problems $\langle u_X'^2 \rangle$ may be expected to exceed the wall normal particle velocity variance, therefore the effect of varying the ratio $\langle u_X'^2 \rangle / \langle u_Y'^2 \rangle$ has to be examined in the future. Two values of the mean tangential incident velocity were tested, namely $\langle u_X \rangle^- = 5\sqrt{\langle u_Y'^2 \rangle^-}$ and $10\sqrt{\langle u_Y'^2 \rangle^-}$.

4.1. Study of the equivalent restitution and friction coefficients

Figs. 5 and 6 illustrate the ratio e^*/e versus the standard deviation of the virtual wall inclination angle σ_γ. In all the plots, the ratio e^*/e is seen to increase with increasing σ_γ, whatever the incident

normal velocity distribution (Gaussian for Fig. 5, uniform for Fig. 6). The slope of the curves increases as the restitution coefficient e decreases, and with increasing value of the mean tangential incident particle velocity, denoting the effect of reducing the mean incidence angle. As can be observed, e^* is always higher than e. Contrary to e, whose maximum value is equal to unity, e^* can reach considerably higher values. This means that the reflected wall normal velocity can significantly exceed the particle impact velocity as soon as roughness is present, since $\langle \tilde{u}_Y \rangle^+ = -e^* \langle u_Y \rangle^-$ (with $\langle u_Y \rangle^- < 0$). Accordingly, the wall normal velocity after collision increases as σ_γ increases. Such a momentum redistribution due to collisions with a rough wall was noticed in earlier works where gas–solid flows were simulated by Lagrangian particle tracking, like the investigations by Fukagata et al. (2001) or Sommerfeld (1995, 2003). As can be observed, the ratio e^*/e is only slightly influenced by the friction coefficient μ, and the effect of the distribution of u_Y is hardly noticeable. Other tests have shown that with increasing values of the tangential incident particle velocity, its influence becomes insignificant.

The evolution of μ^*/μ as a function of the roughness parameter σ_γ is displayed in Figs. 7 and 8. Comparison of these two figures shows that μ^*/μ is almost independent of the distribution of u_Y for a fixed value of the mean tangential incident velocity $\langle u_X \rangle^-$. In contrast to the restitution coefficient, a nonmonotonic behaviour of μ^*/μ is observed, however. The ratio μ^*/μ first decreases with increasing σ_γ, and then it increases. The influence of e dominates in the first part of the curves, in opposite to the second part where the influence of μ is clearly prevailing. Such effects are more obvious when $\langle u_X \rangle^-$ increases. We can observe that the slope change occurs around $\sigma_\gamma \approx 0.05$ for $\langle u_X \rangle^- = 5\sqrt{\langle u_Y'^2 \rangle^-}$ and around $\sigma_\gamma \approx 0.03$ for $\langle u_X \rangle^- = 10\sqrt{\langle u_Y'^2 \rangle^-}$, whatever the friction and restitution coefficients.

The observed behaviours are most likely related to the influence of the shadow effect, which can be characterized by the evolution of the mean value of the virtual wall inclination angle $\langle \gamma \rangle$ as σ_γ

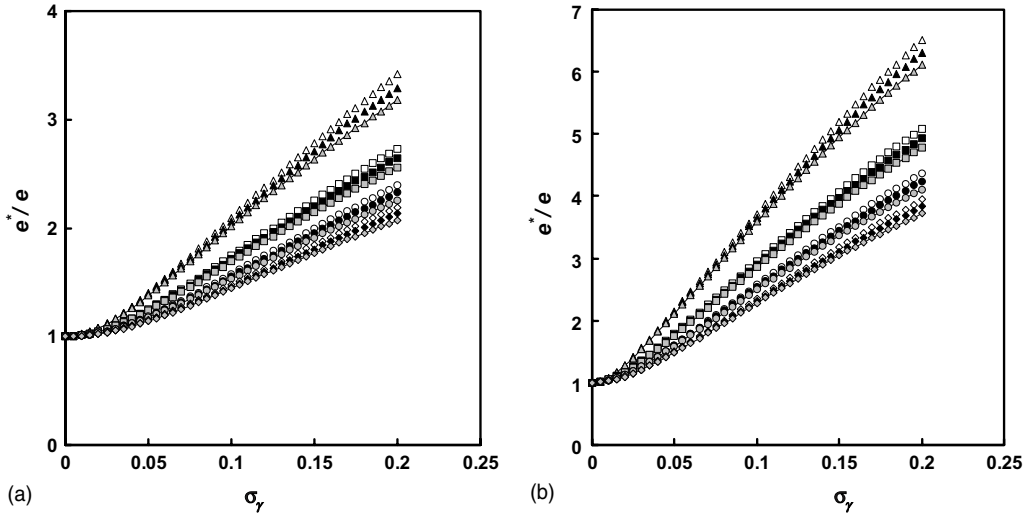

Fig. 5. The ratio e^*/e as a function of the roughness parameter σ_γ for a Gaussian distribution of u_Y. (a) $\langle u_X \rangle^- / \sqrt{\langle u_Y'^2 \rangle^-} = 5$; (b) $\langle u_X \rangle^- / \sqrt{\langle u_Y'^2 \rangle^-} = 10$. $e = 0.4$: (△) $\mu = 0.2$; (▲) $\mu = 0.3$; (-▲-) $\mu = 0.4$, $e = 0.6$: (□) $\mu = 0.2$; (■) $\mu = 0.3$; (-■-) $\mu = 0.4$, $e = 0.8$: (○) $\mu = 0.2$; (●) $\mu = 0.3$; (-●-) $\mu = 0.4$, $e = 1.0$: (◇) $\mu = 0.2$; (◆) $\mu = 0.3$; (-◆-) $\mu = 0.4$.

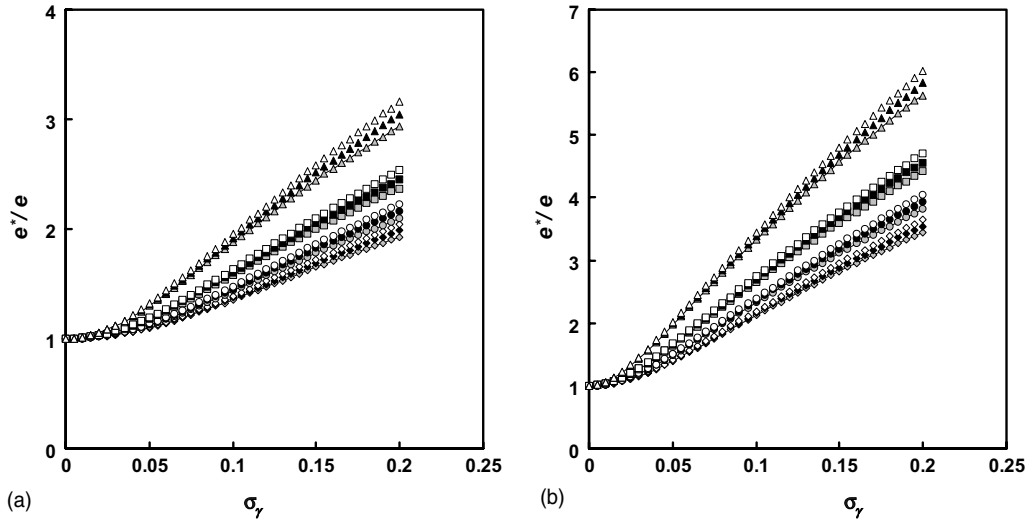

Fig. 6. Same caption as Fig. 5, except uniform distribution of u_Y instead of Gaussian.

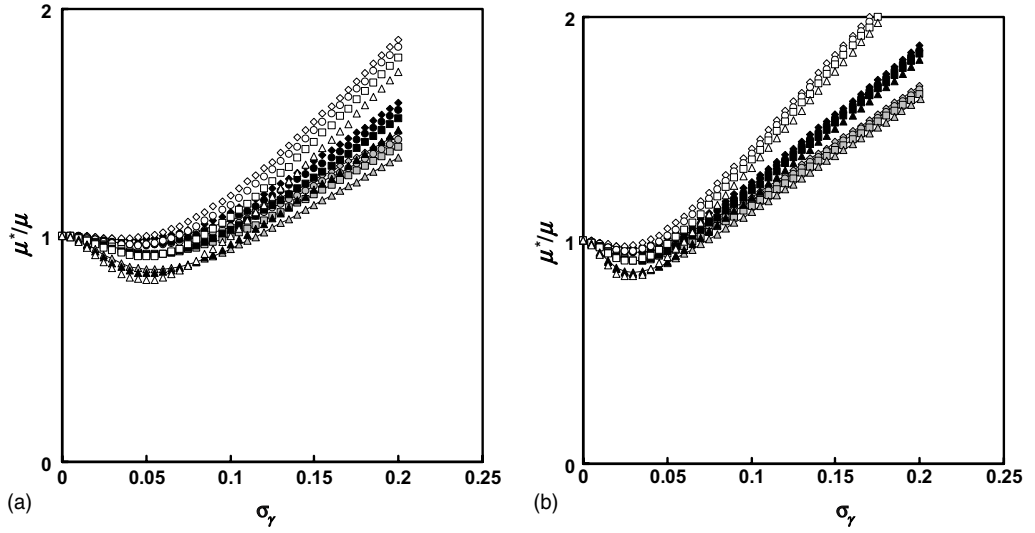

Fig. 7. The ratio μ^*/μ as a function of the roughness parameter σ_γ for a Gaussian distribution of u_Y: (a) $\langle u_X\rangle^-/\sqrt{\langle u_Y'^2\rangle^-} = 5$; (b) $\langle u_X\rangle^-/\sqrt{\langle u_Y'^2\rangle^-} = 10$. Symbol caption as in Fig. 5.

increases. In Fig. 9(a), $\langle\gamma\rangle$ is plotted as a function of σ_γ for the two distributions of u_Y before collision and for the two values of the mean tangential particle velocity $\langle u_X\rangle^-$. Whatever the conditions, the mean value of γ (and therefore the shadow effect) is observed to increase with increasing roughness. For high values of σ_γ, $\langle\gamma\rangle$ varies almost linearly with σ_γ. The shadow effect is seen to be enhanced by larger values of $\langle u_X\rangle^-$, whereas the effect of the distribution of u_Y is very weak. In order to reveal the dependence of the shadow effect on the collision parameters e and μ,

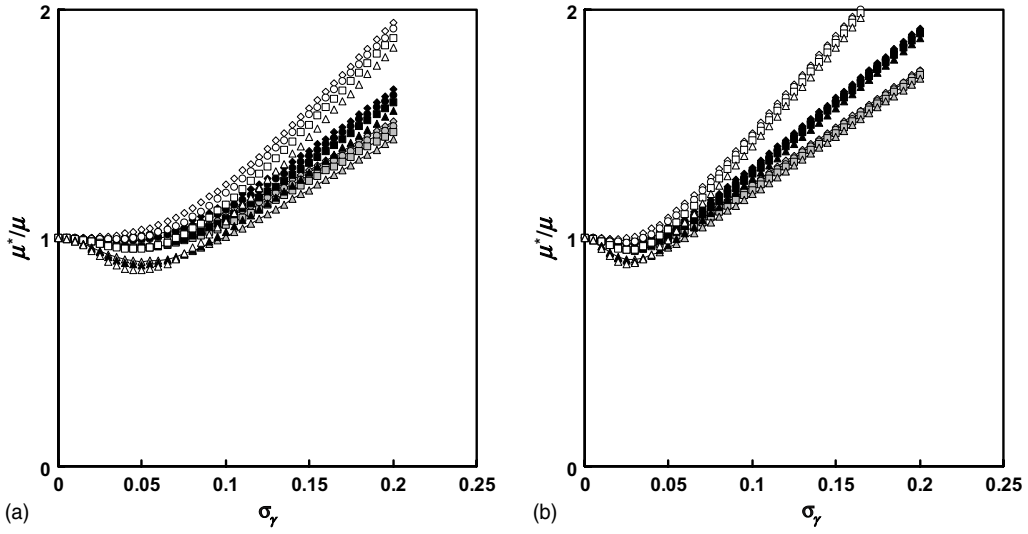

Fig. 8. Same caption as Fig. 7, except uniform distribution of u_Y instead of Gaussian.

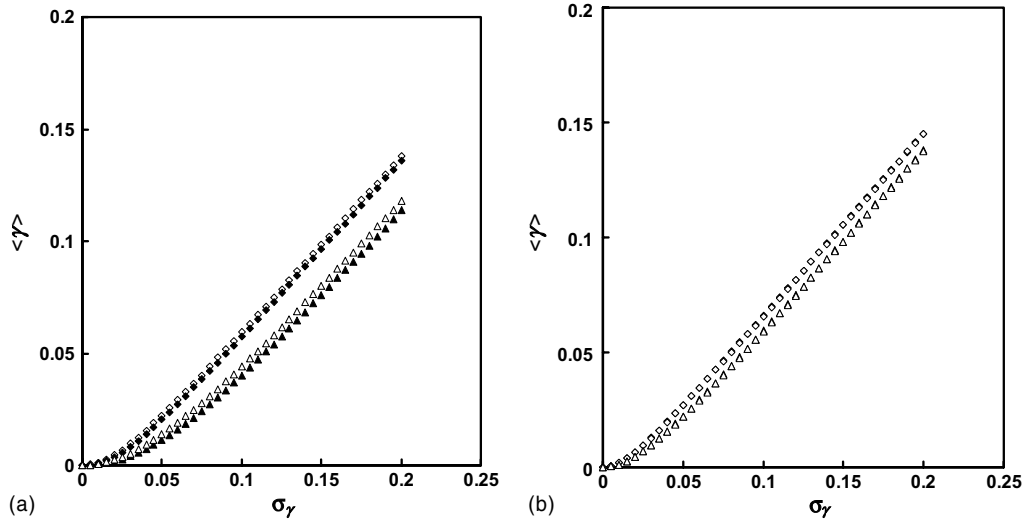

Fig. 9. The shadow effect revealed by the mean value of the inclination angle of the wall, plotted as a function of the roughness parameter σ_γ: (a) Influence of the incident velocity distribution for $e = 0.8$, $\mu = 0.2$. ($\triangle, \blacktriangle$) $\langle u_X\rangle^- / \sqrt{\langle u_Y'^2\rangle^-} = 5$; ($\diamondsuit, \blacklozenge$) $\langle u_X\rangle^- / \sqrt{\langle u_Y'^2\rangle^-} = 10$. Open symbols: Gaussian distribution of u_Y; black symbols: uniform distribution of u_Y. (b) Influence of the Coulomb parameters for a Gaussian distribution of u_Y. $\langle u_X\rangle^- / \sqrt{\langle u_Y'^2\rangle^-} = 5$. $e = 0.4$: $\blacklozenge$ $\mu = 0.2$; $\diamondsuit$ $\mu = 0.4$; $e = 0.8$: $\blacktriangle$ $\mu = 0.2$; $\triangle$ $\mu = 0.4$.

the mean inclination angle $\langle\gamma\rangle$ is displayed in Fig. 9(b) as a function of σ_γ for various values of the restitution and friction coefficients. The results show that the shadow effect does not depend on the friction coefficient, and decreases slightly with increasing e. In that sense, the second part of the curves in Figs. 7 and 8 seems to be almost independent of the shadow effect since the influence

of μ was seen to prevail, contrary to the first part of the curves, for which a small value of e corresponds to a maximum influence of the shadow effect.

This analysis shows that the equivalent parameters e^* and μ^* take into consideration the effects related to the roughness of the wall. Such parameters reproduce, on the one hand, the momentum redistribution of the particle velocity characterized by e^*, which is increasingly large as σ_γ is high, and, on the other hand, the antagonistic effects of μ^*, i.e. a decrease in the equivalent friction for small values of σ_γ (since for such values the momentum redistribution is not yet important) and an increase in μ^* for larger values of σ_γ for which the transverse agitation is important.

4.2. Evaluation of the proposed model

In order to examine the pertinence of the proposed model, the results issuing from the model and from the numerical simulation are compared in Figs. 10–13, in what concerns the normalized third-order velocity correlations defined by

$$\Pi_{YYY} = \frac{\langle u_Y'^3 \rangle}{\langle u_Y'^2 \rangle^{3/2}} \tag{27}$$

shown in Figs. (10) and (11), which should be equal to $C\frac{1-e^*}{\sqrt{e^*}}$ according to the model (26), and

$$\Pi_{XXY} = \frac{\langle u_X'^2 u_Y' \rangle}{\langle u_Y'^2 \rangle^{3/2}} \tag{28}$$

shown in Figs. (12) and (13), which should be equal to $-2\mu^* \langle u_X' u_Y'^2 \rangle - \mu^{*2} \langle u_Y'^3 \rangle$ according to the model (26).

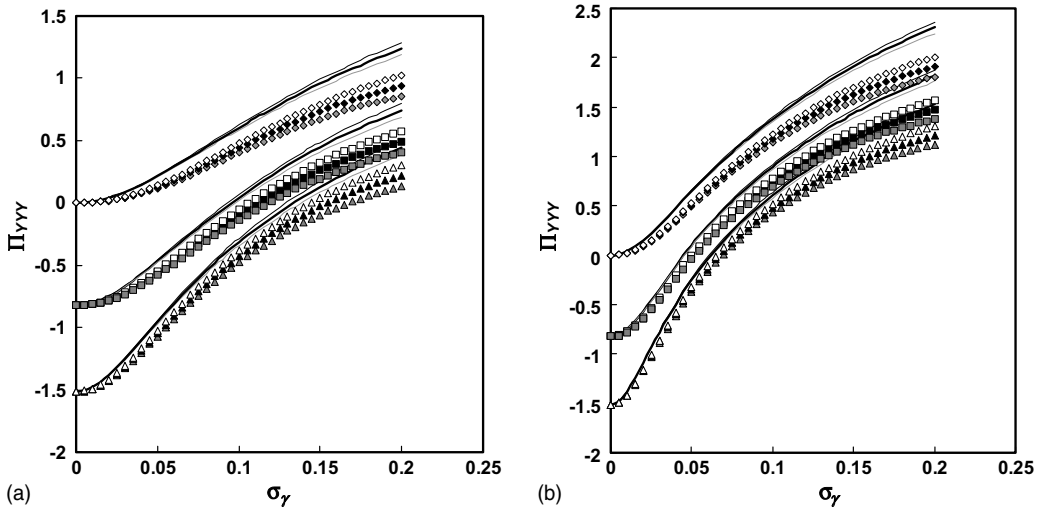

Fig. 10. Comparison between the present model and the numerical results for the normalized third-order velocity correlation Π_{YYY} for a Gaussian distribution of u_Y: (a) $\langle u_X \rangle^- / \sqrt{\langle u_Y'^2 \rangle^-} = 5$; (b) $\langle u_X \rangle^- / \sqrt{\langle u_Y'^2 \rangle^-} = 10$. Lines: model (26). Symbols: numerical simulation. $e = 0.4$: (△) $\mu = 0.2$; (▲) $\mu = 0.3$; (▲) $\mu = 0.4$, $e = 0.6$: (□) $\mu = 0.2$; (■) $\mu = 0.3$; (■) $\mu = 0.4$, $e = 1.0$: (◇) $\mu = 0.2$; (◆) $\mu = 0.3$; (◆) $\mu = 0.4$.

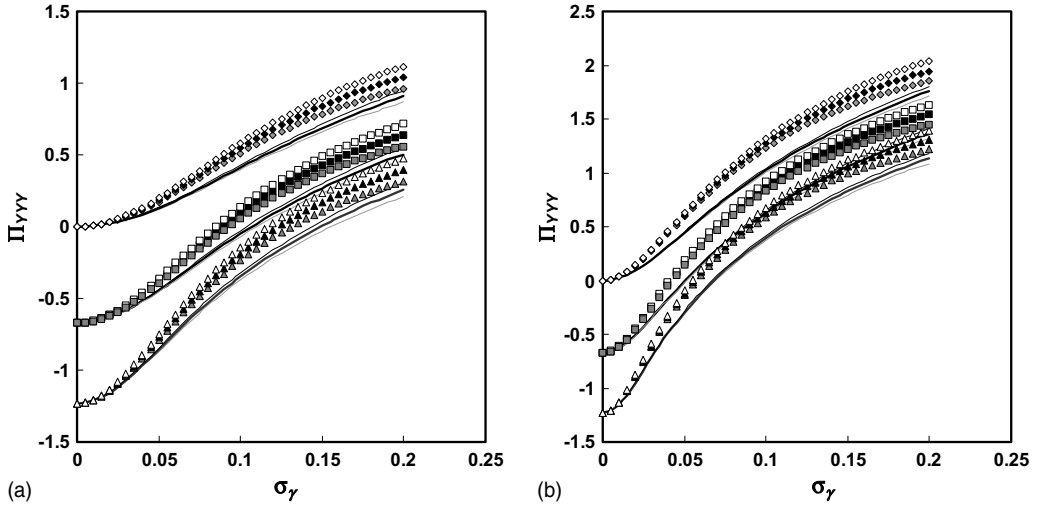

Fig. 11. Same caption as Fig. 10, except uniform distribution of u_Y instead of Gaussian.

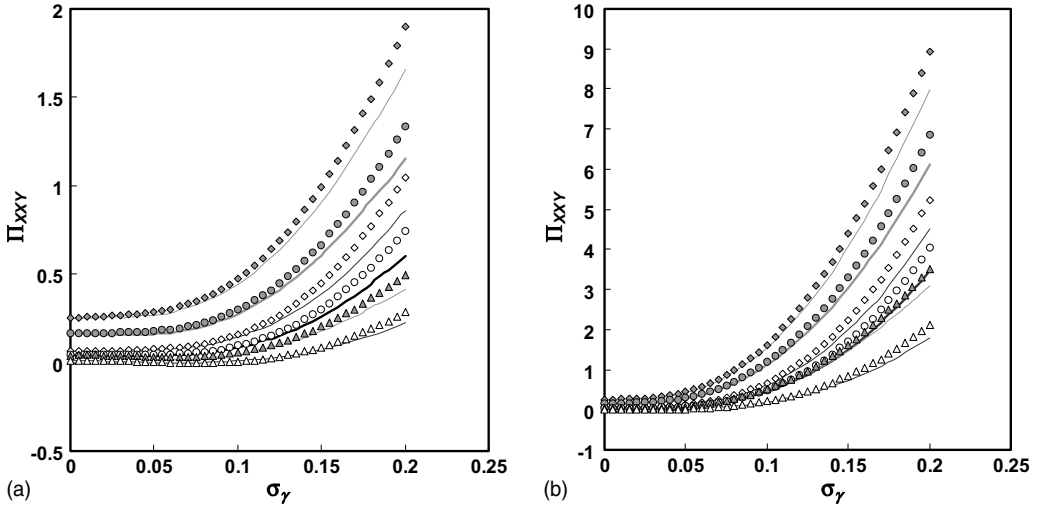

Fig. 12. Comparison between the present model and the numerical results for the normalized third-order velocity correlation Π_{XXY} for a Gaussian distribution of u_Y: (a) $\langle u_X\rangle^-/\sqrt{\langle u_Y'^2\rangle^-} = 5$; (b) $\langle u_X\rangle^-/\sqrt{\langle u_Y'^2\rangle^-} = 10$. Lines: model (26). Symbols: numerical simulation. $e = 0.4$: (△) $\mu = 0.2$; (▲) $\mu = 0.4$, $e = 0.8$: (○) $\mu = 0.2$; (●) $\mu = 0.4$, $e = 1.0$: (◇) $\mu = 0.2$; (◆) $\mu = 0.4$.

In the case of a Gaussian incident normal velocity distribution, even if the model slightly overestimates the computational predictions (Fig. 10), the obtained values are qualitatively in good agreement with the simulations and allow to get a satisfactory estimation of Π_{YYY}. The opposite effect (slight underestimation of Π_{YYY}) is observed when a uniform distribution of u_Y is used, as shown by Fig. 11, whatever the value of the friction and restitution coefficients and whatever the mean tangential incident particle velocity. As can be seen from Figs. 12 and 13,

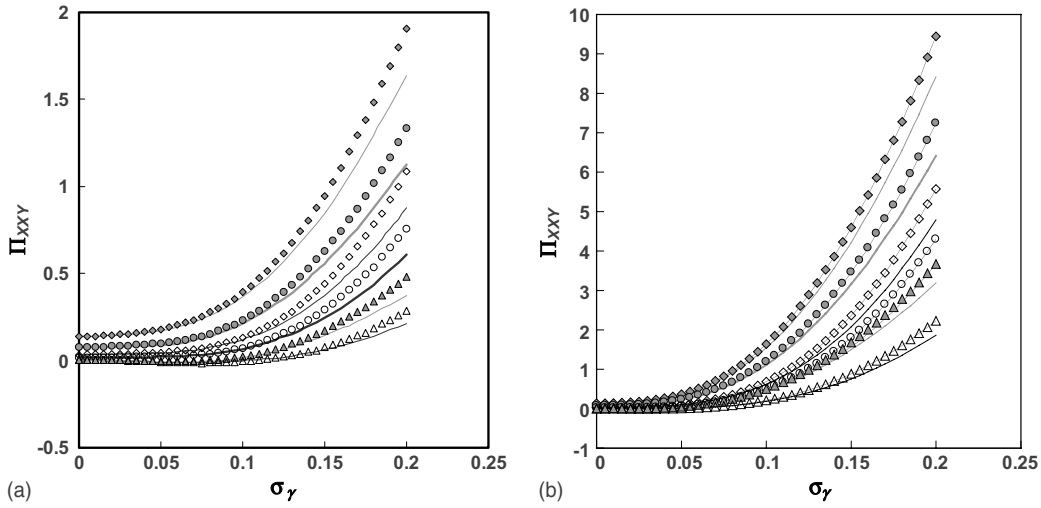

Fig. 13. Same caption as Fig. 12, except uniform distribution of u_Y instead of Gaussian.

better agreement is obtained for the correlation Π_{XXY}, whatever the statistical distribution of u_Y. The correlation Π_{XXY} is slightly underestimated by the model for high values of σ_γ, nevertheless the results are very satisfactory.

To summarize, acceptable estimates of the velocity correlations at the wall are obtained by means of a formulation close to the smooth wall formulation of Sakiz and Simonin (1999), using equivalent restitution and friction coefficients, whose values can be prescribed with the help of Figs. 5 and 6.

5. Conclusions

In order to obtain the boundary conditions needed in two-fluid models for the dispersed phase in case of irregular particle–wall bouncing, a numerical simulation was carried out by computing the particle statistics at the wall, handling the collisions by means of a virtual wall model accounting for the so-called shadow effect. The computational results were analyzed by defining equivalent restitution and friction coefficients (e^*, μ^*) which may be used to replace the original coefficients in the available boundary conditions for smooth wall. The obtained results show that the wall roughness has a considerable influence on the equivalent coefficients whatever the pre-assigned distribution of the incident wall normal particle velocity. Thanks to these new coefficients, a model for the particulate phase boundary conditions is proposed ensuring zero mass flux at the wall. The proposed model leads to good agreement with the results of the numerical simulation.

This preliminary study can be broadened towards more realistic situations by extending the computations beyond the strong limitations of the proposed model, i.e. the two-dimensional character of the bouncing mechanism, and the assumed particle sphericity and isotropy of the particle velocity fluctuations. This could be achieved by taking the spanwise velocity component

into account by means of a three-dimensional roughness model, however it is still not clear how to decide the value of the standard deviation σ_γ in practical problems in order to account for both the particle size (compared to wall roughness) and the actual particle shape in case of departure from sphericity. Additionally, numerical statistical studies in turbulent channel or pipe flows by means of accurate Euler–Lagrange modelling could be performed in order to get a more realistic distribution of the incident wall normal velocity. The boundary conditions involving the particle rotational velocity components could be investigated using the same technique, keeping in mind that the existing two-fluid models are still unable to take the rotational motion of the particle into consideration, however. Finally, the proposed model has to be submitted to a sensitivity study in examining the effects of such boundary conditions on the results provided by two-fluid models in confined gas–solid flows.

Acknowledgements

This work was partly supported by INTAS (grant No. 00-0309), which is gratefully acknowledged.

References

Alipchenkov, V.M., Zaichik, L.I., Simonin, O., 2001. A comparison of two approaches to derivation of boundary conditions for continuous equations of particle motion in turbulent flow. High Temp. 39, 104–110.

Fukagata, K., Zahrai, S., Bark, F., Kondo, S., 2001. Effects of wall roughness in a gas–particle turbulent vertical channel flow. In: Lingborg et al. (Eds.), Proc. 2nd Int. Symp. on Turbulence and Shear Flow Phenomena, vol. II. KTH, Stockholm, pp. 117–122.

He, J., Simonin, O., 1993. Non-equilibrium predictions of the particle phase stress tensor in vertical pneumatic conveying. In: Stock, D. (Ed.), Proc. 5th Int. Symp. on Gas–Solid Flows, ASME Fluids Engineering Division Summer Meeting, Washington, DC, vol. 166. pp. 253–263.

Hyland, K., Simonin, O., Reeks, M.W., 1998. On the continuum equations for two-phase flows. In: Proc. 3rd Int. Conf. on Multiphase Flow, ICMF'98, Lyon, France. Paper No. 567.

Reeks, M.W., 1993. On the constitutive relations for dispersed particles in non-uniform flows. 1: dispersion in a simple shear flow. Phys. Fluids A 5 (3), 750–761.

Sakiz, M., Simonin, O., 1999. Development and validation of continuum particle wall boundary conditions using Lagrangian simulation of a vertical gas–solid channel flow. In: Proc. 3rd ASME/JSME Joint Fluids Eng. Conf., San-Francisco, CA. Paper No. 7898.

Schade, K.P., Hadrich, Th., 1998. Investigation of influence of wall roughness on particle–wall collisions. In: Proc. 3rd Int. Conf. on Multiphase Flow, ICMF'98, Lyon, France. Paper No. 250.

Simonin, O., Deutsch, E., Boivin, M., 1993. Large eddy simulation and second-moment closure model of particle fluctuating motion in two-phase turbulent shear flows. In: Proc. 9th Int. Symp. on Turbulent Shear Flows, Kyoto, Japan. pp. 85–115 (published by Springer-Verlag, 1995).

Sommerfeld, M., 1992. Modelling of particle/wall collisions in confined gas–particle flows. Int. J. Multiphase Flow 18, 905–926.

Sommerfeld, M., 1995. The importance of inter-particle collisions in horizontal gas–solid channel flows. In: Proc. ASME Fluids Engineering Division Conference, vol. 228. Hiltons Head, pp. 335–345.

Sommerfeld, M., 2002. Kinetic simulations for analysing the wall collision process of non-spherical particles. In: Proc. ASME Fluids Engineering Division Summer Meeting, Montreal, Canada, Paper No. 31239.

Sommerfeld, M., 2003. Analysis of collision effects for turbulent gas–particle flow in a horizontal channel: Part I. Particle transport. Int. J. Multiphase Flow 29, 675–699.

Sommerfeld, M., Huber, N., 1999. Experimental analysis and modelling of particle–wall collisions. Int. J. Multiphase Flow 25, 1457–1489.

Sommerfeld, M., Zivkovic, G., 1992. Recent advances in the numerical simulation of pneumatic conveying trough pipe systems. In: Hirsch, Ch., Periaux, J., Onate, E. (Eds.), Computational Methods in Applied Science. In: Invited Lectures and Special Technological Sessions of the First European Computational Fluid Dynamics Conference and the First Conference on Numerical Methods in Engineering, Brussels. pp. 201–212.

Tsuji, Y., Morikawa, Y., Tanaka, T., Nakatsukasa, N., Nakatami, M., 1987. Numerical simulation of gas–solid two phase flow in a two dimensional horizontal channel. Int. J. Multiphase Flow 13, 671–684.

Tsuji, Y., Oshima, T., Morikawa, Y., 1985. Numerical simulation of pneumatic conveying in a horizontal pipe. KONA, Powder Science & Technology in Japan 3, 38–51.

Zhang, X., Zhou, L.X., 2002. A two-fluid particle–wall collision model accounting for the wall roughness. In: Sommerfeld, M. (Ed.), Proc. 10th Workshop on Two-Phase Flow Predictions, Merseburg, Germany. pp. 44–51.

Zhou, L.X., Chen, T., Li, Y., Xu, Y., Gu, H.X., Zheng, C.G., Liu, Z.H., Yu, Y., 2001. Recent advances in the second-order moment two-phase turbulence models for gas–particle and bubble-liquid flows. In: Proc. 4th Int. Conf. on Multiphase Flow, ICMF'2001, New Orleans, LA. Paper No. 602.